Geosystems and Geoenvironment 3 (2024) 100242

Contents lists available at ScienceDirect

Geosystems and Geoenvironment

journal homepage: www.elsevier.com/locate/geogeo

Scaling laws in the evolutionary processes of marine animals over the last 540 million years

Haitao Shang

Institute of Ecology and Evolution, University of Oregon, OR 97403, USA

ARTICLE INFO

Article history:
Received 31 March 2023
Revised 23 September 2023
Accepted 12 October 2023

Handling Editor: Sanzhong Li

Keywords:
Scaling law
Variation rate
Marine animals
Phanerozoic Eon
Evolutionary processes
Biodiversity
Origination intensity
Extinction intensity
Body size

ABSTRACT

Scaling laws are ubiquitous in modern biological systems. However, whether such patterns existed in deep-time biological systems is less investigated; the best-known example is the scaling law between the frequency and size of extinction events. Here, I show that the variation rates of biodiversity, origination intensity, extinction intensity, and body size of marine animals during the last 540 million years exhibited scaling laws. I then derive a general form of these scaling laws from a conceptual model with some principles of thermodynamics and assumptions about the global biological system. The results in this study suggest that the scaling laws systematically appearing in the biological metrics characterizing different aspects of the evolutionary processes of marine animals likely belong to the same universality class and probably derived from a set of common factors.

1. Introduction

The Phanerozoic, which spans from 540 million years ago (Ma) to the present, is a distinctive episode in the evolutionary history of life. Fossil record, especially that of marine animals (Sepkoski, 2002), provides a window through which to investigate the patterns and underlying mechanisms of life's evolution in this eon. Biological matrices, including biodiversity (i.e., the number of distinct genera alive at any given geologic time), origination intensity (i.e., the percentage of genera in their first appearance), and extinction intensity (i.e., the percentage of genera in their last appearance), have been used to quantitatively characterize different aspects of the evolutionary processes. Fig. 1a–c show the time series of biodiversity, origination intensity, and extinction intensity of the Phanerozoic marine animals, respectively. Studies on these time series have suggested that the evolutionary processes of marine animals over the last 540 million years exhibited a variety of dynamical properties, including cyclicity (Raup and Sepkoski, 1984; Rohde and Muller, 2005), contingency (Blount et al., 2018; Gould, 1989), and punctuated equilibrium (Eldredge, 1989; Gould, 2002; Gould and Eldredge, 1977). The other metric that has attracted much attention is the body size (Fig. 1d), which is tightly correlated with organisms' physiological and ecological traits (Clauset and Erwin, 2008; Gillooly et al., 2005; Heim et al., 2015). Investigating how body sizes changed in the past is crucial for understanding the biotic adaptation and responses to global environmental changes (Butterfield, 2011; Holland and Sclafani, 2015).

The scaling law is expressed as $y \propto x^{\lambda}$, where x and y are two variables and λ is the scaling exponent (Bak, 2013; Schroeder, 2009). On a log-log plot, this mathematical expression can be rewritten as $\log_{10} y \propto \lambda \log_{10} x$, which indicates that the underlying mechanisms regulating this relation do not depend on specific scales (Bak, 2013; Schroeder, 2009). Scale-invariant behaviors are widespread in modern biological systems and have been intensively investigated (Bak, 2013; Schroeder, 2009). Scaling laws in ancient biological systems, nevertheless, are understudied; the most famous example is the scaling law of frequency versus size of extinction events (Newman, 1997; Raup, 1986). However, whether scale-invariant behaviors existed in the variation rates of deep-time evolutionary processes remains unclear.

Here, I show that the variation rates of biodiversity, origination intensity, extinction intensity, and body size of marine animals during the last 540 million years exhibited scaling laws. With some basic principles of physics and assumptions about macroscopic biological systems, I suggest a conceptual model that may offer an interpretation for the scaling laws appearing in the evolutionary processes of Phanerozoic marine animals from

E-mail address: htshang.research@gmail.com

https://doi.org/10.1016/j.geogeo.2023.100242

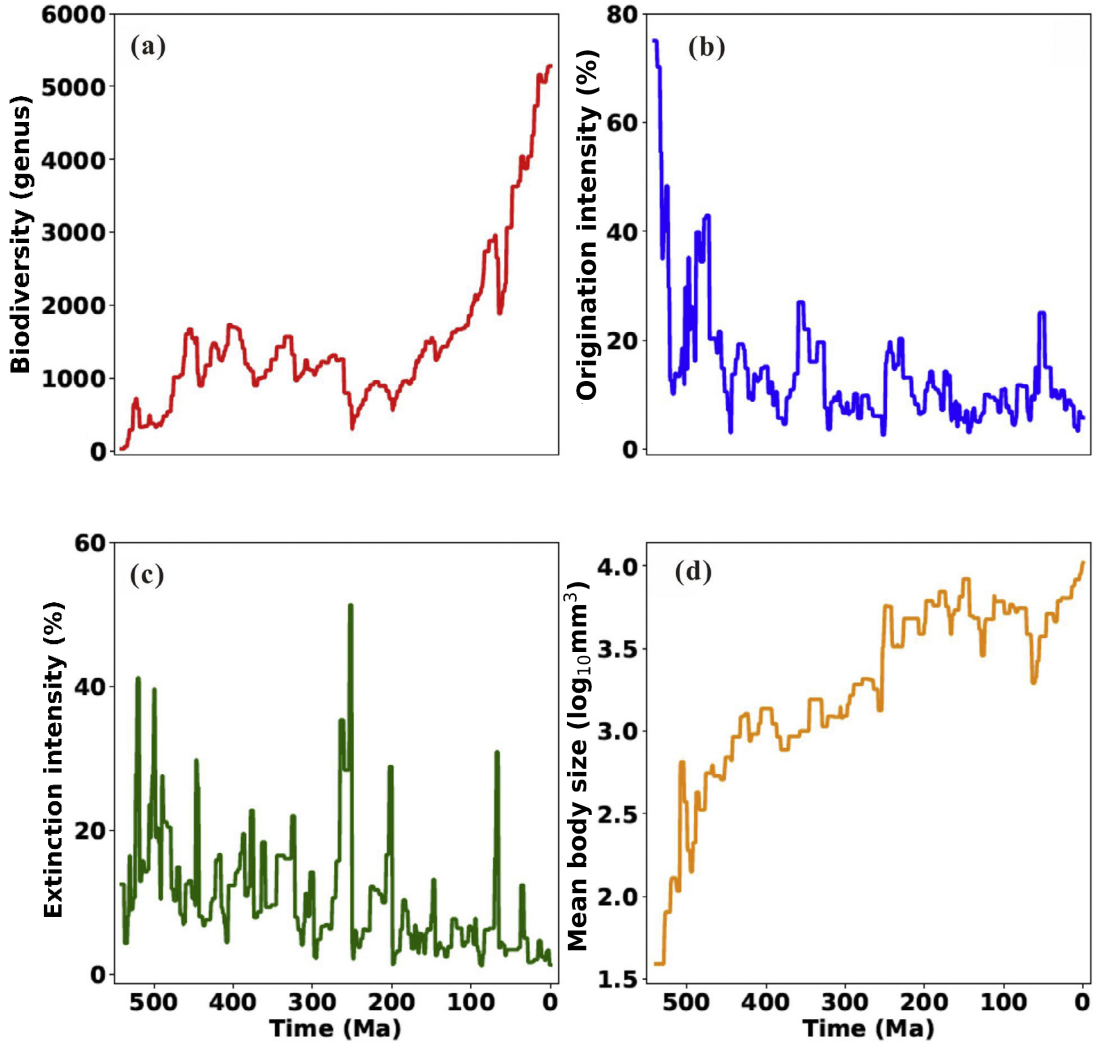

Fig. 1. Time series of (a) biodiversity, (b) origination intensity, (c) extinction intensity, and (d) mean body size of marine animals over the last 540 million years. The unit of time is million years ago (Ma). The datasets on biodiversity, origination intensity, and extinction intensity are from Sepkoski's compendium (Sepkoski, 2002) updated by Rohde and Muller (2005), and the dataset on the mean body size is from the study by Heim et al. (2015).

the perspective of thermodynamics. The scale-invariant patterns illustrated in this study manifest the intrinsic dynamics of the global biological system at geologic timescales.

2. Methods and materials

2.1. Data processing and fitting

The time series of marine animals' biodiversity, origination intensity, and extinction intensity over the last 540 million years are from Sepkoski's compendium (Sepkoski, 2002) updated by Rohde and Muller (2005). Original data points in these three time series are evenly spaced with the time step of 1 million years. The time series of Phanerozoic marine animals' body sizes is from the study by Heim et al. (2015). Original data points in this time series are at the stage level; in other words, time intervals have varying lengths. I group these data points of body sizes into bins with the width of 1 million year and calculate the mean in each bin. Each of these four datasets (biodiversity, origination intensity, extinction intensity, and body size) therefore contains 540 data points. To better investigate scaling laws, which generally span several orders of magnitude, I interpolate each dataset with different types of splines including the smoothing (De Boor, 2001), regression (Friedman, 1991), and penalized (Ruppert, 2002) splines. The penalized spline turns out to fit the four datasets better than the smoothing and regression splines. I then compute the value at every 0.1 million years of each time series with its best-fitting penalized spline; each dataset used in the following analyses therefore contains 5400 data points.

To investigate the variation rates in these datasets, I first denote one time series as $\{S(t)\}$, where $S(t)$ is the data value at time t. I then calculate the difference between the data values at every two consecutive time points (i.e., $S(t+\Delta t)$ and $S(t)$, where Δt is the time step) and denote this difference as $\Delta S_t = S(t+\Delta t) - S(t)$. The variation rate therefore is expressed as

$$r_t = \frac{\Delta S_t}{\Delta t} \tag{1}$$

I classify the variation rates (i.e., r_t's) into three categories: negative ($r_t < 0$), positive ($r_t > 0$), and all ($r_t \neq 0$), denoted by r^{N}, r^{P}, and r^{A}, respectively. Logarithms of negative values are mathematically undefined; values of the data in these three categories, denoted by $|\mathrm{r}^{\mathrm{N}}| = \{|r_t| : \ t_t < 0\}$, $|\mathrm{r}^{\mathrm{P}}| = \{|r_t| : \ t_t > 0\}$, and $|\mathrm{r}^{\mathrm{A}}| = \{|r_t| : \ t_t \neq 0\}$, are used to investigate the scaling laws. Zero values of r_t's are not used in the following analysis because the logarithm of a zero is undefined in mathematics.

According to Sturges' Rule (Scott, 2009), the optimal number of bins (N_{bin}) for a dataset depends on the specific number of data points (N_{data}) in it and is determined using $N_{\text{bin}} = \log_2(N_{\text{data}})+1$. I denote the number of data points in each category of $|r^{\text{N}}|$, $|r^{\text{P}}|$, and $|r^{\text{A}}|$ by $N_{\text{data,N}}$, $N_{\text{data,P}}$, and $N_{\text{data,A}}$, respectively; the optimal numbers of bins for these three categories therefore are $N_{\text{bin},N}=\log_2(N_{\text{data,N}})+1$, $N_{\text{bin},P}=\log_2(N_{\text{data,P}})+1$, and $N_{\text{bin},A}=\log_2(N_{\text{data,A}})+1$, respectively. The count (i.e., the number of data points) in the j-th bin is denoted by N_j, and the bins with no data points are discarded. The total number of bins used for the following analyses (after discarding the empty bins) is denoted by J; the set $\{N_0, N_1, \cdots, N_J\}$ is henceforth denoted by $\{N_j\}_{j=0}^{J}$. A key property of scaling laws is their right tails, where large values of random variables appear; the initial values on the left side of the distribution sometimes do not follow a scaling law and thus should not be used for data fitting (Alstott et al., 2014; Clauset et al., 2009). To identify the place to truncate the set of counts $\{N_j\}_{j=0}^{J}$, one needs to determine the point where the scaling behavior starts to appear; this truncation point is henceforth denoted as $N_{\min}$. To determine the location of $N_{\min}$, I establish a scaling-law fit starting from each individual data point in $\{N_j\}_{j=0}^{J}$ and then choose the point generating the minimum value for the distance between the fit and the data as the optimal truncation point (Alstott et al., 2014; Clauset et al., 2009). More specifically, I denote the subset of $\{N_j\}_{j=0}^{J}$ that starts from the point N_p by $I_p = \{N_j\}_{j=p}^{J} = \{N_p, N_{p+1}, \cdots, N_J\}$, fit data points in each of these subsets (i.e., I_0, I_1, $\cdots$, I_{J-1}) on log-log plots, and calculate the error (denoted by ϵ_p) between the data and the fit for each subset (Alstott et al., 2014; Clauset et al., 2009). I denote the minimum error for all subsets as $\epsilon_{\min} = \min\{\epsilon_p\}$. The subset I_p corresponding to $\epsilon_{\min}$ is the optimal subset for the scaling-law fitting and is denoted by $I_{p,\text{opt}}$; the initial point in $I_{p,\text{opt}}$ is the optimal truncation point $N_{\min}$ mentioned above. Therefore, $N_{\text{counts,opt}} = \{N_{\min}, \cdots, N_J\}$ is the truncated set of counts used for data fitting.

2.2. Goodness-of-fit tests

To evaluate the goodness of fit of scaling laws, I calculate the coefficients of determination (R^2's) and root mean square errors (RMSEs) and perform the Kolmogorov-Smirnov (KS) test (Massey, 1951) and Cramér-von Mises (CM) two-sample test (Anderson, 1962). The metric R^2 measures the fraction of variations in the dependent variable N that can be predicted from the independent variable $|r|$ using the best-fitting scaling laws; a larger value of R^2 indicates a better fitting and therefore a more reliable model (Freund and Wilson, 2014). The RMSE, a widely used statistical metric characterizing the accuracy of a model, measures the average difference between actual and predicted values; a smaller value of RMSE suggests a better model. The mathematical definition of the KS statistic is $\max|G_{\text{data}} - G_{\text{model}}|$, which measures the maximum distance between the cumulative distribution functions (CDFs) of the scaling law best fitting the data (G_{model}) and the data themselves (G_{data}) (Massey, 1951). The mathematical definition of the CM test is $\frac{P\times Q}{(P+Q)^2}\left(\sum_{p=0}^{P}[G_{\text{model}}(x_p)-G_{\text{data}}(x_p)]^2+\sum_{q=0}^{Q}[G_{\text{model}}(x'_q)-G_{\text{data}}(x'_q)]^2\right)$, where $\{x_p\}_{p=0}^{P}$ and $\{x'_q\}_{q=0}^{Q}$ are samples independently drawn from two distributions with G_{model} and G_{data}, respectively (Anderson, 1962). Here, I test the null hypothesis, $H_0: G_{\text{model}} = G_{\text{data}}$, against the two-sided alternative, $H_1: G_{\text{model}} \neq G_{\text{data}}$. Following the convention, I set the critical p-value for the KS and CM tests as 0.05; $p > 0.05$ suggests that a scaling law fits the data well while $p \leq 0.05$ indicates that a scaling law does not adequately describe the data.

2.3. Likelihood-ratio tests

To compare the fitting result of the best scaling law for each dataset to those of other heavy-tailed processes (e.g., stretched exponential and lognormal distributions) that are able to produce scaling law-like distributions, I perform the likelihood-ratio test (Clauset et al., 2009): $R = \log(\mathcal{L}_{\text{A}} / \mathcal{L}_{\text{B}})$, where $\mathcal{L}_{\text{A}}$ and $\mathcal{L}_{\text{B}}$ are the likelihoods under the hypothesis of type-A and type-B distributions, respectively. If $R > 0$, then the model fitted using the type-A distribution outperforms the model fitted using the type-B distribution; however, if $R < 0$, then the model fitted with type-B distribution prevails. To correct for random fluctuations, I standardize R by the standard deviation (Clauset et al., 2009; Vuong, 1989), which yields a p-value for determining whether the sign of R is statistically significant or not. I set the significance level for the p-value as 0.05. If $p > 0.05$, then the sign of R is inconclusive and one fails to conclude that one distribution outperforms the other for the given dataset; however, if $p \leq 0.05$, then the sign of R is unlikely to derive from random fluctuations and thus indicates that one distribution fits the given dataset better than the other.

3. Results and discussion

3.1. Scaling laws

The variation rates of the four biological metrics characterizing the evolutionary processes of marine animals during the last 540 million years–biodiversity, origination intensity, extinction intensity, and body size–are classified into three categories: negative ($|r^{\text{N}}|$), positive ($|r^{\text{P}}|$), and all ($|r^{\text{A}}|$), which are defined in Section 2.1. Fig. 2 shows the scaling behaviors of the variation rates in the three categories of each variable. The mathematical expressions of the best-fitting scaling laws and the values of their R^2's and RMSEs are presented in Table 1. To evaluate the goodness of fit of these scaling laws, I also perform the KS and CM tests and compute their p-values, which are denoted by p_{KS} and p_{CM}, respectively. The results (Table 1) show that the p-values of these tests are all much larger than the critical threshold of 0.05 (Section 2.2), suggesting that the scaling laws presented in Table 1 fit the data well. As a property of scaling laws, a straight line on a log-log graph is a necessary but not sufficient condition for the existence of a scaling law. Due to sampling fluctuations, other heavy-tailed processes, such as stretched exponential and lognormal distributions, may generate datasets with distributions that are close to scaling laws (Alstott et al., 2014; Clauset et al., 2009). To compare the best-fitting scaling laws to other heavy-tailed distributions, I conduct the likelihood-ratio test (Section 2.3) and find that the best-fitting scaling laws obtained here outperform exponential, stretched exponential, and lognormal distributions for the datasets on the variation rates.

3.2. A conceptual model for the scaling laws of variation rates in evolutionary processes

Biodiversity, origination intensity, extinction intensity, and body size characterize different aspects of the evolutionary processes of Phanerozoic marine animals; their variation rates therefore should manifest the dynamics of the global biological system. In Section 2.1, I denote the realizations of one biological quantity (i.e., biodiversity, origination intensity, extinction intensity, or body size) at two consecutive time points as $S(t)$ and $S(t+\Delta t)$, where Δt is a constant time step. The variation rates of these biological quantities are defined in Eq. (1). For simplicity, I assume in the

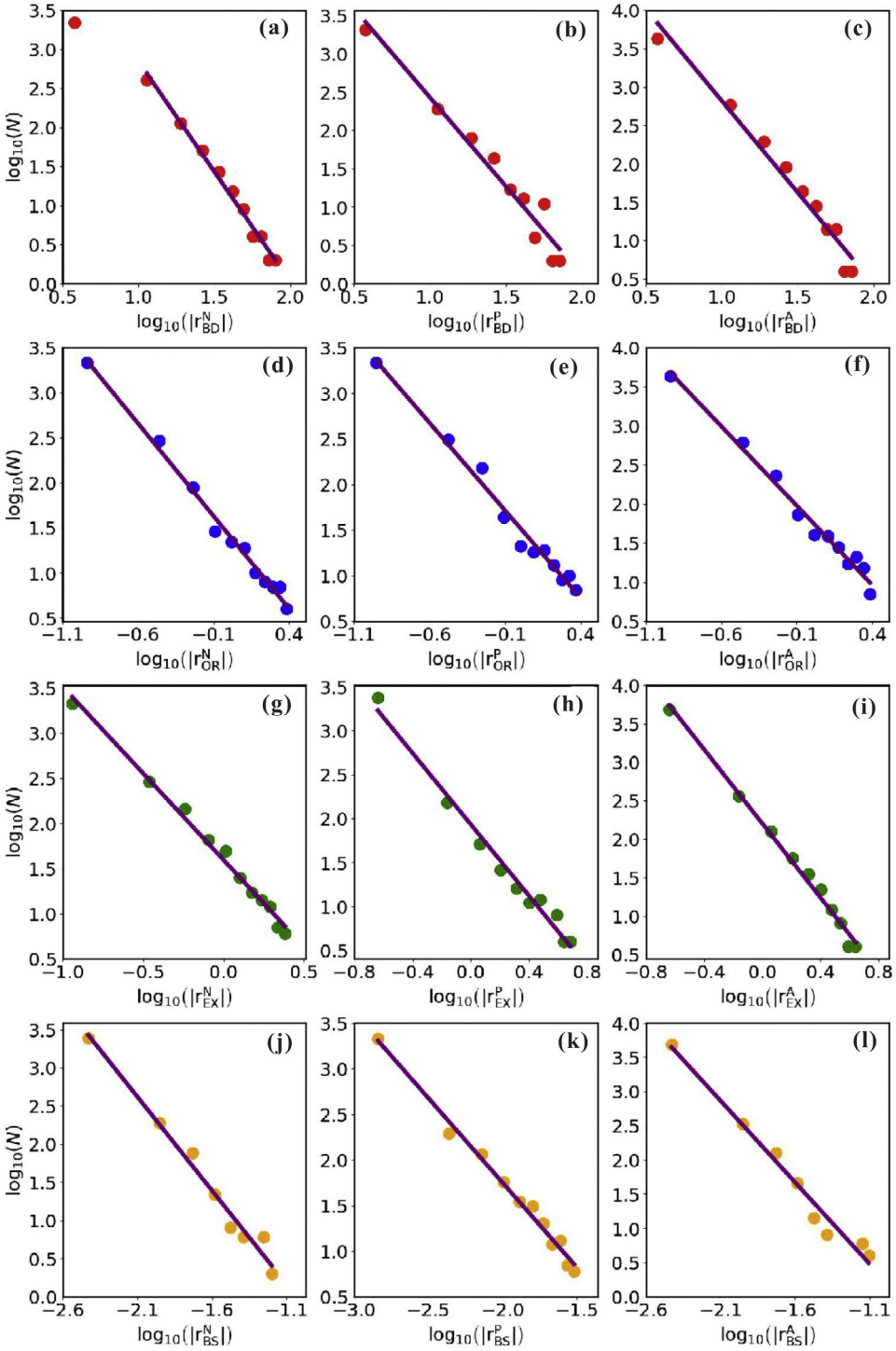

Fig. 2. Scaling laws of negative variation rates ($|r^N|$), positive variation rates ($|r^P|$), and all variation rates ($|r^A|$) in (a – c) biodiversity (BD), (d – f) origination intensity (OR), (g – i) extinction intensity (EX), and (j – l) body size (BS) of marine animals during the last 540 million years. Red, blue, green, and orange circles represent the variation rates (i.e., r_t's defined in Section 2.1) versus counts (i.e., N's) for biodiversity, origination intensity, extinction intensity, and body size, respectively. The initial value in panel (a) that does not follow the scaling law is not included in data fitting (Section 2.1). Purple lines are the best-fitting scaling laws (i.e., least-squares fitting of data on log-log plots) for variation rates in each category of the four biological metrics.

following derivation that $S(t) < S(t+\Delta t)$ so that both ΔS_t and r_t are positive for all t and therefore both $\log(\Delta S_t)$ and $\log(r_t)$ are always mathematically well-defined. For the case of $S(t+\Delta t) < S(t)$, in which $\Delta S_t < 0$ and $r_t < 0$, one can obtain the same general form of the scaling laws (that is, Eq. (11)) by replacing ΔS_t and r_t with $|\Delta S_t|$ and $|r_t|$, respectively, in the following derivation (refer to the definitions for the three categories of variation rates $|r^N|$, $|r^P|$, and $|r^A|$ in Section 2.1). I do not consider the case of $S(t+\Delta t) = S(t)$ here because the logarithms of $\Delta S_t = 0$ and $r_t = 0$ are undefined in mathematics (Section 2.1).

The entropies of the biological system at the states corresponding to the realizations $S(t)$ and $S(t+\Delta t)$ are $E(S(t)) = -\log p(S(t))$ and $E(S(t+\Delta t)) = -\log p(S(t+\Delta t))$, where $p(S(t))$ is the probability that the realization $S(t)$ occurs and $E(S(t))$ char-

Table 1
Scaling laws of negative variation rates ($|\mathbf{r^N}|$), positive variation rates ($|\mathbf{r^P}|$), and all variation rates ($|\mathbf{r^A}|$) in biodiversity (BD), origination intensity (OR), extinction intensity (EX), and body size (BS) of marine animals during the last 540 million years. The R^2, RMSE, p_{KS}, and p_{CM} represent the coefficient of determination, root mean square error, the p-value of the KS test, and the p-value of the CM test, respectively, of the least-squares fitting on log-log plots.

Variable	Category	Best-fitting scaling law	R^2	RMSE	p_{KS}	p_{CM}
Biodiversity	Negative	$N \sim \lvert r^N_{BD}\rvert^{-2.42}$	0.87	0.17	0.99	0.93
	Positive	$N \sim \lvert r^P_{BD}\rvert^{-2.31}$	0.99	0.04	1.00	0.96
	All	$N \sim \lvert r^A_{BD}\rvert^{-2.39}$	0.96	0.10	1.00	0.96
Origination intensity	Negative	$N \sim \lvert r^N_{OR}\rvert^{-2.10}$	0.91	0.17	0.99	0.81
	Positive	$N \sim \lvert r^P_{OR}\rvert^{-2.02}$	0.84	0.23	0.99	0.74
	All	$N \sim \lvert r^A_{OR}\rvert^{-2.06}$	0.90	0.18	0.99	0.95
Extinction intensity	Negative	$N \sim \lvert r^N_{EX}\rvert^{-2.12}$	0.92	0.14	0.99	0.97
	Positive	$N \sim \lvert r^P_{EX}\rvert^{-2.03}$	0.91	0.17	0.99	0.96
	All	$N \sim \lvert r^A_{EX}\rvert^{-2.41}$	0.97	0.11	0.99	1.00
Body size	Negative	$N \sim \lvert r^N_{BS}\rvert^{-2.46}$	0.83	0.16	1.00	1.00
	Positive	$N \sim \lvert r^P_{BS}\rvert^{-2.05}$	0.69	0.17	0.96	0.85
	All	$N \sim \lvert r^A_{BS}\rvert^{-2.39}$	0.93	0.07	1.00	1.00

acterizes the deviation of the biological system's state at realization $S(t)$ from the equilibrium. When the quantity of interest switches from $S(t)$ to $S(t+\Delta t)$, the corresponding change in the entropy of the system is $\Delta E_t = E(S(t+\Delta t)) - E(S(t))$. Based on the additivity of entropy (Almeida, 2003; Skilling, 1989), this change in entropy corresponding to ΔS_t can be rewritten as

$$\Delta E_t = E(S(t+\Delta t) - S(t)) = -\log p(\Delta S_t). \tag{2}$$

Since ΔE_t in Eq. (2) is a function of $p(\Delta S_t)$, the mean of ΔE_t over all t can be expressed as

$$\langle \Delta E_t \rangle = \sum_t p(\Delta S_t) \cdot \log p(\Delta S_t) \tag{3}$$

in which $\langle \cdot \rangle$ represents the mean of a quantity. Since the time step Δt is constant, I obtain the following relations from Eq. (1):

$$p(r_t) \sim p(\Delta S_t) \text{ and } \log p(r_t) \sim \log p(\Delta S_t). \tag{4}$$

I substitute Eq. (4) into Eq. (3) and obtain

$$\langle \Delta E_t \rangle \sim \sum_t p(r_t) \cdot \log p(r_t) \tag{5}$$

where the probability $p(r_t)$ satisfies the following normalizing condition:

$$\sum_t p(r_t) = 1. \tag{6}$$

The Gaia hypothesis suggests that the interactions between geological and biological processes have shaped the Earth system into a stable, habitable environment (Lenton, 1998; Lovelock, 2000). Due to the regulation of a variety of feedback mechanisms, the Earth-life system is generally balanced over geologic timescales (Lenton, 1998; Lovelock, 2000). The structures of complex systems, such as the Earth-life system, are usually located at certain intermediate levels between perfect disorder and perfect order (Anderson, 1972; Prigogine, 1980); the order of magnitude of quantities may better characterize the complexity and variability of the global biological system than their specific values. According to the steady-state evolution suggested by the Gaia hypothesis (Lenton, 1998; Lovelock, 2000), I assume that the average variation in the global biological system is maintained at a certain order of magnitude: $\sum_t p(\Delta S_t) \cdot \mathcal{O}(\Delta S_t) \simeq \phi$, where $\mathcal{O}(\Delta S_t) \sim \log(\Delta S_t)$ represents the order of magnitude of ΔS_t and ϕ is a constant. Since $p(r_t) \sim p(\Delta S_t)$ (Eq. (4)) and $\log r_t \sim \log(\Delta S_t)$ (Eq. (1)), I obtain

$$\sum_t p(r_t) \cdot \log r_t \simeq \phi. \tag{7}$$

While the Earth system is stabilized by the interactions between life and the environment Lenton, 1998; Lovelock, 2000), the dissipative nature of individual physical and biological processes tends to drive the Earth system and its components away from steady states, resulting in fluctuations around equilibria (Kleidon, 2010; Vallino and Algar, 2016). From the perspective of thermodynamics, the maximum entropy production principle proposes that a nonlinear dynamical system with a high degree of freedom, such as the global biological system, tends to select the state that maximizes the change in entropy (under some external constraints) along its evolutionary trajectory (Dewar, 2005; Kleidon and Lorenz, 2005; Martyushev, 2010). In light of this principle, I calculate the maximum of the average change in entropy, $\langle \Delta E_t \rangle$ in Eq. (5), under the constraints of Eqs. (6) and ((7). To do so, I first express the Lagrangian (Jaynes, 1957) as

$$\mathcal{L} = -\sum_t p(r_t) \cdot \log\ p(r_t) + \mu\left(\sum_t p(r_t) - 1\right) + \lambda\left(\sum_t p(r_t) \cdot \log r_t - \phi\right) \tag{8}$$

where real numbers μ and λ are Lagrangian multipliers. Taking the derivative of $\mathcal{L}$ in Eq. (8) with respect to $p(r_t)$ gives

$$\frac{\partial \mathcal{L}}{\partial p(r_t)} = -\big(\log\ p(r_t) + 1\big) + \mu + \lambda\ \log r_t. \tag{9}$$

When $\partial \mathcal{L}/\partial p(r_t) = 0$ (i.e., the right-hand side of Eq. (9) equals 0), I obtain

$$p(r_t) = \exp\,(\mu - 1) \cdot r_t^{\lambda}. \tag{10}$$

If one takes X measurements, the number of times that the variation rates with the value r_t appear can be expressed as $N(r_t) = X \cdot p(r_t)$. Eq. (10) then implies that the relation between $N(r_t)$ and r_t follows

$$N(r_t) \sim r_t^{\lambda}. \tag{11}$$

which is a general form of the scaling laws illustrated in Fig. 2 and Table 1.

3.3. Implications

The scaling behaviors in the variation rates of biodiversity, origination intensity, extinction intensity, and body size (Fig. 2 and Table 1) suggest that large variation rates were much less frequent than small ones in the evolutionary processes of marine animals over the last 540 million years and that the mechanisms responsible for these variation rates did not depend on specific scales (Bak, 2013; Schroeder, 2009). Fig. 3 summarizes the exponents (λ's; circles) of these scaling laws. The mean value and standard deviation of these exponents are $\mu_\lambda = -2.23$ (horizontal purple line in Fig. 3) and $\sigma_\lambda = 0.17$, respectively. The coefficient of variation (i.e., the ratio of the standard deviation to the absolute value

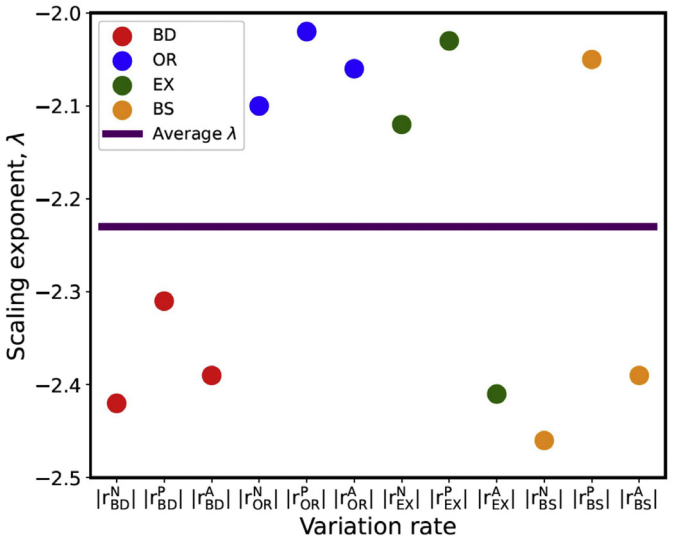

Fig. 3. Exponents (λ's) of scaling laws for the variation rates of biodiversity ($|r^N_{BD}|$, $|r^P_{BD}|$, and $|r^A_{BD}|$), origination intensity ($|r^N_{OR}|$, $|r^P_{OR}|$, and $|r^A_{OR}|$), extinction intensity ($|r^N_{EX}|$, $|r^P_{EX}|$, and $|r^A_{EX}|$), and body size ($|r^N_{BS}|$, $|r^P_{BS}|$, and $|r^A_{BS}|$) of marine animals over the last 540 million years. Red, blue, green, and orange circles represent the exponents of scaling laws for the variation rates of biodiversity, origination intensity, extinction intensity, and body size, respectively. Horizontal purple line represents the mean of all exponents.

of the mean) equals $\sigma_\lambda/|\mu_\lambda| = 7.62\%$, suggesting that the variations in these scaling exponents are rather small relative to μ_λ. In statistical mechanics, two systems possessing the same scaling-law functions and identical exponents belong to the same universality class (Stanley, 1999; Stanley et al., 2000). The almost identical scaling exponents observed in this study (Fig. 3) imply that the variation rates of the four biological metrics are in the same universality class.

The exponents of many identified scaling laws in natural systems are between −3.0 and −2.0, indicating that the means of these scaling laws are well-defined while their variances are not (Clauset et al., 2009; Newman, 2005). Such well-defined means but ill-defined variances suggest that "black swan events" might have appeared in the evolutionary processes of Phanerozoic marine animals (Taleb, 2016). Black swan events refer to the rare and unexpected events that have extraordinarily large magnitude and play significant roles in the dynamical behaviors of a system (Taleb, 2016). In this study, the exponents of all scaling laws (Fig. 2 and Table 1) are between −2.5 and −2.0 (Fig. 3), implying the existence of "black swan events" in the four biological metrics, which is consistent with the occasional but significant radiations and extinctions of life during the last 540 million years (Bush and Payne, 2021; Butterfield, 2011; Raup, 1986).

Scaling behaviors systematically appear in the variation rates of biodiversity, origination intensity, extinction intensity, and body size, suggesting that certain fundamental and universal mechanisms may be responsible for such patterns. Nevertheless, similar to many identified scaling laws in complex systems, the factors drove the evolutionary processes of Phanerozoic marine animals to exhibit scaling laws remain unknown. Studies have proposed that the evolution of marine animals was remarkably influenced by a variety of environmental variables. For instance, the concentration of dissolved O_2 in seawater significantly affects metabolisms (Deutsch et al., 2020, 2015), impacting the biodiversity, origination intensity, extinction intensity, and body size of marine animals (Decker and Van Holde, 2011; Payne et al., 2020). Another example is Earth's surface temperature, which remarkably influences the physiology of life (Deutsch et al., 2020, 2015) and has been shown to be strongly correlated with the four biological metrics (Mayhew et al., 2012; Song et al., 2021). Whether and how these environmental variables and the interactions among them might have resulted in the systemic scaling behaviors observed here require future investigation.

As mentioned above, the most well-known scaling law in paleobiology is the one between the frequency and size of extinction events (Bak, 2013; Raup, 1986). Various theories have been proposed to interpret this scaling law, such as the NK model of Kauffman and Johnsen (1991), the percolation model of Plotnick and McKinney (1993), and the self-organized criticality (SOC) model of Bak and Sneppen (1993). The NK model (Kauffman and Johnsen, 1991) focuses on the evolution of coupled fitness landscapes, the percolation model (Plotnick and McKinney, 1993) investigates the impact of changes in the behaviors and ranges of some species on others, and the SOC model (Bak and Sneppen, 1993) describes the dynamical patterns of species evolving on a fitness landscape. Nevertheless, statistical analyses on fossil data have suggested that the exponent of the scaling law for the frequency versus size of extinction events is around 2 (Newman, 1996; Solé and Bascompte, 1996), which rules out the NK (Kauffman and Johnsen, 1991) and percolation (Plotnick and McKinney, 1993) models because both of them predict a scaling exponent in the vicinity of 1 (Newman, 1997). Moreover, a scaling law is neither a necessary nor a sufficient condition for SOC (Solow, 2005; Touboul and Destexhe, 2017). The origin of the scaling law of extinction sizes remains an open question; other theories, such as the random stress model of Newman (1997) and the highly optimized tolerance mechanism of Carlson and Doyle (1999), also offer plausible interpretations but need further justification.

Different from previous studies focusing on the scaling law between the frequency and size of extinction events, this work shows that the variation rates of biodiversity, origination intensity, extinction intensity, and body size of marine animals over the last 540 million years exhibited scaling laws as well. With some basic principles of thermodynamics and assumptions about the global biological system, I derive a conceptual model linking variation rates to entropy and use this model to derive a general form of these scaling laws. However, the theory proposed in this study does not offer explanations for why the exponents of the scaling laws in Table 1 take those specific values and what factors affect them; these remaining questions require more exploration. Moreover, for any open natural system, theoretical models are not unique (Oreskes et al., 1994); more general and fundamental theoretical interpretations for these scaling laws are expected to be suggested by future work.

Declaration of Competing Interest

The author declares no known competing financial interests or personal relationships that could have appeared to influence the work reported in this paper.

CRediT authorship contribution statement

Haitao Shang: Investigation, Project administration, Conceptualization, Data curation, Formal analysis, Methodology, Resources, Software, Supervision, Validation, Visualization, Writing – original draft, Writing – review & editing.

Acknowledgments

I thank Editor Sanzhong Li for securing reviewers for the manuscript and two anonymous reviewers for thoughtful and constructive comments.

References

Almeida, M.P., 2003. Thermodynamical entropy (and its additivity) within generalized thermodynamics. Phys. A Stat. Mech. Appl. 325, 426–438. doi:10.1016/S0378-4371(03)00262-0.

Alstott, J., Bullmore, E., Plenz, D., 2014. Powerlaw: A python package for analysis of heavy-tailed distributions. PLoS One 9, e85777. doi:10.1371/journal.pone.0085777.

Anderson, P.W., 1972. More Is different: Broken symmetry and the nature of the hierarchical structure of science. Science 177, 393–396. doi:10.1126/science.177.4047.393.

Anderson, T.W., 1962. On the distribution of the two-sample Cramér-von Mises criterion. Ann. Math. Stat. 33, 1148–1159. doi:10.1214/aoms/1177704477.

Bak, P., 2013. How Nature Works: the Science of Self-Organized Criticality. Springer, New York.

Bak, P., Sneppen, K., 1993. Punctuated equilibrium and criticality in a simple model of evolution. Phys. Rev. Lett. 71, 4083–4086. doi:10.1103/PhysRevLett.71.4083.

Blount, Z.D., Lenski, R.E., Losos, J.B., 2018. Contingency and determinism in evolution: Replaying life's tape. Science 362, eaam5979. doi:10.1126/science.aam5979.

Bush, A.M., Payne, J.L., 2021. Biotic and abiotic controls on the Phanerozoic history of marine animal biodiversity. Annu. Rev. Ecol. Evol. Syst. 52, 269–289. doi:10.1146/annurev-ecolsys-012021-035131.

Butterfield, N.J., 2011. Animals and the invention of the Phanerozoic Earth system. Trends Ecol. Evol. 26, 81–87. doi:10.1016/j.tree.2010.11.012.

Carlson, J.M., Doyle, J., 1999. Highly optimized tolerance: A mechanism for power laws in designed systems. Phys. Rev. E 60, 1412–1427. doi:10.1103/PhysRevE.60.1412.

Clauset, A., Erwin, D.H., 2008. The evolution and distribution of species body size. Science 321, 399–401. doi:10.1126/science.1157534.

Clauset, A., Shalizi, C.R., Newman, M.E.J., 2009. Power-law distributions in empirical data. SIAM Rev. 51, 661–703. doi:10.1137/070710111.

De Boor, C., 2001. A Practical Guide to Splines. Springer, New York.

Decker, H., Van Holde, K.E., 2011. Oxygen and the Evolution of Life. Springer, Heidelberg doi:10.1007/978-3-642-13179-0.

Deutsch, C., Ferrel, A., Seibel, B., Pörtner, H.O., Huey, R.B., 2015. Climate change tightens a metabolic constraint on marine habitats. Science 348, 1132–1135. doi:10.1126/science.aaa1605.

Deutsch, C., Penn, J.L., Seibel, B., 2020. Metabolic trait diversity shapes marine biogeography. Nature 585, 557–562. doi:10.1038/s41586-020-2721-y.

Dewar, R.C., 2005. Maximum entropy production and the fluctuation theorem. J. Phys. Math. Gen. 38, L371–L381. doi:10.1088/0305-4470/38/21/L01.

Eldredge, N., 1989. Time Frames: The Evolution of Punctuated Equilibria. Princeton University Press, New Jersey.

Freund, R.J., Wilson, W.J., 2014. Statistical Methods. Elsevier Science, Burlington.

Friedman, J.H., 1991. Multivariate adaptive regression splines. Ann. Stat. 19. doi:10.1214/aos/1176347963.

Gillooly, J.F., Allen, A.P., West, G.B., Brown, J.H., 2005. The rate of DNA evolution: Effects of body size and temperature on the molecular clock. Proc. Natl. Acad. Sci 102, 140–145. doi:10.1073/pnas.0407735101.

Gould, S.J., 2002. The Structure of Evolutionary Theory. Harvard University Press, Massachusetts doi:10.4159/9780674417922.

Gould, S.J., 1989. Wonderful Life: The Burgess Shale and the Nature of History. W.W. Norton, New York.

Gould, S.J., Eldredge, N., 1977. Punctuated equilibria: The tempo and mode of evolution reconsidered. Paleobiology 3, 115–151. doi:10.1017/S0094837300005224.

Heim, N.A., Knope, M.L., Schaal, E.K., Wang, S.C., Payne, J.L., 2015. Cope's rule in the evolution of marine animals. Science 347, 867–870. doi:10.1126/science.1260065.

Holland, S.M., Sclafani, J.A., 2015. Phanerozoic diversity and neutral theory. Paleobiology 41, 369–376. doi:10.1017/pab.2015.10.

Jaynes, E.T., 1957. Information theory and statistical mechanics. Phys. Rev. 106, 620–630. doi:10.1103/PhysRev.106.620.

Kauffman, S.A., Johnsen, S., 1991. Coevolution to the edge of chaos: Coupled fitness landscapes, poised states, and coevolutionary avalanches. J. Theor. Biol. 149, 467–505. doi:10.1016/S0022-5193(05)80094-3.

Kleidon, A., 2010. A basic introduction to the thermodynamics of the Earth system far from equilibrium and maximum entropy production. Philos. Trans. R. Soc. B Biol. Sci. 365, 1303–1315. doi:10.1098/rstb.2009.0310.

Kleidon, A., Lorenz, R., 2005. Non-Equilibrium Thermodynamics and the Production of Entropy: Life, Earth, and Beyond, Understanding Complex Systems. Springer,, New York.

Lenton, T.M., 1998. Gaia and natural selection. Nature 394, 439–447. doi:10.1038/28792.

Lovelock, J., 2000. Gaia: A New Look at Life on Earth. Oxford University Press, Oxford.

Martyushev, L.M., 2010. The maximum entropy production principle: Two basic questions. Philos. Trans. R. Soc. B Biol. Sci. 365, 1333–1334. doi:10.1098/rstb.2009.0295.

Massey, F.J., 1951. The Kolmogorov-Smirnov test for goodness of fit. J. Am. Stat. Assoc. 46, 68–78. doi:10.1080/01621459.1951.10500769.

Mayhew, P.J., Bell, M.A., Benton, T.G., McGowan, A.J., 2012. Biodiversity tracks temperature over time. Proc. Natl. Acad. Sci 109, 15141–15145.

Newman, M., 2005. Power laws, Pareto distributions and Zipf's law. Contemp. Phys. 46, 323–351. doi:10.1080/00107510500052444.

Newman, M.E.J., 1997. A model of mass extinction. J. Theor. Biol. 189, 235–252. doi:10.1006/jtbi.1997.0508.

Newman, M.E.J., 1996. Self-organized criticality, evolution and the fossil extinction record. Proc. R. Soc. Lond. B Biol. Sci. 263, 1605–1610. doi:10.1098/rspb.1996.0235.

Oreskes, N., Shrader-Frechette, K., Belitz, K., 1994. Verification, validation, and confirmation of numerical models in the Earth sciences. Science 263, 641–646. doi:10.1126/science.263.5147.641.

Payne, J.L., Bachan, A., Heim, N.A., Hull, P.M., Knope, M.L., 2020. The evolution of complex life and the stabilization of the Earth system. Interface Focus 10, 20190106. doi:10.1098/rsfs.2019.0106.

Plotnick, R.E., McKinney, M.L., 1993. Ecosystem organization and extinction dynamics. Palaios 8, 202. doi:10.2307/3515172.

Prigogine, I., 1980. From Being to Becoming: Time and Complexity in the Physical Sciences. W. H. Freeman, San Francisco.

Raup, D.M., 1986. Biological extinction in Earth history. Science 231, 1528–1533. doi:10.1126/science.11542058.

Raup, D.M., Sepkoski, J.J., 1984. Periodicity of extinctions in the geologic past. Proc. Natl. Acad. Sci. 81 (3), 801–805.

Rohde, R.A., Muller, R.A., 2005. Cycles in fossil diversity. Nature 434 (7030), 208–210.

Ruppert, D., 2002. Selecting the number of knots for penalized splines. J. Comput. Graph. Stat. 11, 735–757. doi:10.1198/106186002853.

Schroeder, M.R., 2009. Fractals, Chaos, Power laws: Minutes from an Infinite Paradise. Dover Publications,, New York.

Scott, D.W., 2009. Sturges' rule. Wiley Interdiscip. Rev. Comput. Stat. 1, 303–306. doi:10.1002/wics.35.

Sepkoski, J.J., 2002. A compendium of fossil marine animal genera. In: Bulletins of American Paleontology, 203, pp. 1–560.

Skilling, J., Skilling, J., 1989. Classic maximum entropy. In: Maximum Entropy and Bayesian Methods. Springer, Netherlands, pp. 45–52. doi:10.1007/978-94-015-7860-8_3.

Solé, R., Bascompte, J., 1996. Are critical phenomena relevant to large-scale evolution? Proc. R. Soc. Lond. B Biol. Sci. 263, 161–168. doi:10.1098/rspb.1996.0026.

Solow, A.R., 2005. Power laws without complexity. Ecol. Lett. 8, 361–363.

Song, H., Kemp, D.B., Tian, L., Chu, D., Song, H., Dai, X., 2021. Thresholds of temperature change for mass extinctions. Nature Communications 12 (1), 1–8.

Stanley, H.E., 1999. Scaling, universality, and renormalization: Three pillars of modern critical phenomena. Rev. Mod. Phys. 71, S358–S366. doi:10.1103/RevModPhys.71.S358.

Stanley, H.E., Amaral, L.A.N., Gopikrishnan, P., Ivanov, P.C., Keitt, T.H., Plerou, V., 2000. Scale invariance and universality: Organizing principles in complex systems. Phys. A Stat. Mech. Appl. 281, 60–68. doi:10.1016/S0378-4371(00)00195-3.

Taleb, N.N., 2016. The Black Swan: The Impact of the Highly Improbable. Random House, New York.

Touboul, J., Destexhe, A., 2017. Power-law statistics and universal scaling in the absence of criticality. Phys. Rev. E 95, 012413.

Vallino, J.J., Algar, C.K., 2016. The thermodynamics of marine biogeochemical cycles: Lotka revisited. Annu. Rev. Mar. Sci. 8, 333–356. doi:10.1146/annurev-marine-010814-015843.

Vuong, Q.H., 1989. Likelihood ratio tests for model selection and non-nested hypotheses. Econometrica 57, 307. doi:10.2307/1912557.